Wnt Signals and Frizzled Activity Orient Anterior-Posterior Axon Outgrowth in *C. elegans*

Massimo A. Hilliard[1] and Cornelia I. Bargmann[1,*]
[1] Howard Hughes Medical Institute and
Laboratory of Neural Circuits and Behavior
The Rockefeller University
1230 York Avenue
New York, New York 10025

Summary

Secreted proteins of the Wnt family affect axon guidance, asymmetric cell division, and cell fate. We show here that *C. elegans* Wnts acting through Frizzled receptors can shape axon and dendrite trajectories by reversing the anterior-posterior polarity of neurons. In *lin-44/Wnt* and *lin-17/Frizzled* mutants, the polarity of the PLM mechanosensory neuron is reversed along the body axis: the long PLM process, PLM growth cone, and synapses are posterior to its cell body instead of anterior. Similarly, the polarity of the ALM mechanosensory neuron is reversed in *cwn-1 egl-20* Wnt double mutants, suggesting that different Wnt signals regulate neuronal polarity at different anterior-posterior positions. LIN-17 protein is asymmetrically localized to the posterior process of PLM in a *lin-44*-dependent manner, indicating that Wnt signaling redistributes LIN-17 in PLM. In this context, Wnts appear to function not as instructive growth cone attractants or repellents, but as organizers of neuronal polarity.

Introduction

Many developing neurons extend processes along the anterior-posterior or dorsal-ventral body axis. In both vertebrates and invertebrates, guidance of cells and axons along the dorsal-ventral axis is mediated by the secreted guidance factors Netrin and Slit (Hedgecock et al., 1990; Ishii et al., 1992; Kennedy et al., 1994; Harris et al., 1996; Kidd et al., 1999; Brose et al., 1999; Hao et al., 2001). The cues for anterior-posterior, or longitudinal, guidance are only now being discovered. Secreted proteins of the Wnt family, which were long known to affect cell fates, were first suggested to have a role in longitudinal guidance in studies of neuroblast cell migration in *C. elegans*. The Wnt EGL-20 regulates migration of the two Q neuroblasts QL and QR, which are born just anterior to the major site of *egl-20* expression in the tail (Harris et al., 1996; Maloof et al., 1999; Whangbo and Kenyon, 1999). EGL-20 promotes the posterior migration of QL neuroblasts by inducing expression of a Hox gene that respecifies their cell fates. EGL-20 also regulates the anterior guidance of QR neuroblasts and their descendants, but this pathway does not appear to involve new gene expression. Instead, EGL-20 promotes the ability of QR to follow positional information along the longitudinal body axis. Ubiquitous expression of *egl-20* can rescue its QR migration defects, suggesting that

egl-20 is not the sole source of anterior-posterior information for QR (Whangbo and Kenyon, 1999).

Many guidance factors have roles in both cell and axon migrations, and, similarly, Wnt proteins and their Frizzled and Ryk receptors have recently been implicated in axon guidance. In contrast with the permissive role proposed for *egl-20* in cell migration, the Wnts in *Drosophila* and mice are thought to provide instructive attractive and repulsive cues to axonal growth cones. In *Drosophila*, Wnt5 expressed in the posterior commissure of each segment acts as a repellent; axons expressing the Ryk-like receptor Derailed only cross the ventral midline through the anterior commissure (Yoshikawa et al., 2003). In mice, vertebrate corticospinal neurons that express a Ryk protein grow posteriorly and are repelled by Wnts (Liu et al., 2005). In an opposite, attractive role for Wnts, mouse Wnt4 acts as an anterior attractant for commissural axons after they have crossed the midline; Frizzled3 is the Wnt receptor that allows commissural axons to follow the head-to-tail Wnt gradient in the spinal cord (Lyuksyutova et al., 2003).

The *C. elegans* genome contains five Wnt ligands (*lin-44*, *egl-20*, *cwn-1*, *cwn-2*, *mom-2*), four Frizzled receptors (*lin-17*, *mig-1*, *cfz-2*, *mom-5*), and one homolog of Ryk/Derailed (*lin-18*). In *C. elegans*, Wnt proteins and their receptors have a central role in orienting the polarity of many asymmetric cell divisions (Sternberg and Horvitz, 1988; Herman and Horvitz, 1994; Herman et al., 1995; Sawa et al., 1996; Whangbo et al., 2000; Inoue et al., 2004). Interestingly, these cell divisions are invariably asymmetric along the anterior-posterior body axis (Lin et al., 1998). The asymmetric cell divisions often involve both new gene expression and an intracellular reorganization of the receptor-expressing cell. For example, at the four-cell stage of development, the Wnt ligand MOM-2 produced by the posterior P2 cell signals to the MOM-5 Frizzled receptor on the EMS blastomere; this signal reorients the EMS mitotic spindle and induces the endodermal fate in one EMS daughter (Thorpe et al., 1997). Endodermal induction involves transcription and a cell fate change, but mitotic spindle rotation is independent of new gene expression, indicating that the Wnt/Fz signal can polarize intracellular structures in EMS (Schlesinger et al., 1999).

The idea that Wnt/Fz signaling can reorient existing cellular structures finds further support from studies of planar cell polarity, or PCP. PCP describes the ability of Frizzled signaling to orient fields of cells along a common axis, as is seen in the beautiful, ordered patterns of eye facets and wing hairs in *Drosophila* (Gubb and Garcia-Bellido, 1982; Vinson and Adler, 1987; Vinson et al., 1989; Bhanot et al., 1996; Bhat, 1998; Kennerdell and Carthew, 1998; Chen and Struhl, 1999; Zheng et al., 1995; Wehrli and Tomlinson 1995, 1998). During PCP, interactions between adjacent cells drive Frizzled protein to one edge of each cell, defining an intracellular axis of asymmetry that is oriented with respect to extracellular landmarks such as the distal edge of the wing (Strutt, 2001). In vertebrates, Wnt/Fz pathways with similarity to PCP are used to orient the stereocilia of auditory hair

*Correspondence: cori@rockefeller.edu

cells and the migration of cells during convergent extension (Heisenberg et al., 2000; Guo et al., 2004; Ishikawa et al., 2001).

Many neurons in *C. elegans* send axons along the anterior-posterior axis. Here, we show that the anterior-posterior axon growth of *C. elegans* PLM mechanosensory neurons is regulated by Wnt (*lin-44*) and Frizzled (*lin-17*) signaling. However, the Wnt LIN-44 does not act as a traditional attractant or repellent for PLM growth cones. Instead, Wnt signaling drives a complete inversion of PLM neuronal polarity along the body axis. Two other Wnts, *cwn-1* and *egl-20*, have a similar role in the development of ALM mechanosensory neurons in a different part of the body. These results reveal a surprising analogy between the role of Wnts in cell polarization during asymmetric cell division and the role of Wnts in developing neurons.

Results

lin-17 and *lin-44* Mutations Disrupt Anterior-Posterior PLM Process Outgrowth

The left and right PLM neurons are bipolar mechanosensory neurons whose cell bodies reside in the posterior lumbar ganglion (White et al., 1986). Two processes extend from each PLM cell body—a long anterior process that extends to the center of the animals and a short posterior process that extends part of the distance to the tail (Figures 1A and 1B). The two processes are functionally distinct. The anterior process makes all synapses; it forms gap junctions near its cell body and chemical synapses from a ventral branch near its anterior end. The posterior process does not form synapses or branches.

To identify signaling proteins involved in anterior-posterior axon guidance, we examined PLM neurons in candidate mutants by using the *mec-4::GFP* transgene *zdIs5*. Interesting defects were observed in the Wnt mutant *lin-44* and in the Frizzled mutant *lin-17*. In both *lin-44* and *lin-17* mutant animals, the PLM anterior process was severely shortened, typically extending about 50 μm instead of ∼250–300 μm from the cell body (Figures 1C and 1D; premature termination of PLM in *lin-17* was independently noted by Ch'ng et al. [2003]). By contrast, the posterior PLM process in *lin-17* and *lin-44* mutants extended at least twice as far as it did in the wild-type (∼100 μm instead of ∼15–30 μm), and it usually extended all the way to the end of the tail. In some cases, the posterior process turned at the end of the tail and extended anteriorly, reaching a length similar to that of a wild-type anterior process (Figure 1E).

The defects in PLM were highly penetrant in three strong *lin-17* alleles and one strong *lin-44* allele (Figure 1F). The PLM axon defects of *lin-44 lin-17* double mutants were qualitatively and quantitatively similar to those observed in the single *lin-17* or *lin-44* mutants (Figure 1F). These genetic results suggest that *lin-44* and *lin-17* act in the same process to affect PLM development.

PLM defects were not observed in animals mutant for *mig-1* and *cfz-2*, two other *C. elegans* Frizzled homologs, or in animals mutant for the Wnt ligands *egl-20*, *cwn-1*, and *cwn-2* (Figures 1F and 1G, and data not shown). *egl-20* and *cwn-1* do have a minor role in PLM development: a mutation in *egl-20* enhanced the PLM defect

of *lin-44* animals, and in the triple Wnt mutant *lin-44 cwn-1 egl-20*, almost all PLM neurons were defective (Figure 1G).

Reporter genes for mechanosensory neurons are appropriately expressed in *lin-44* mutants, but about 40% of *lin-17* mutants have extra PLM neurons (see Experimental Procedures and Figure S1; see the Supplemental Data available with this article online). The PLM duplications cannot explain the polarity defect in PLM, since polarity reversals were equally frequent in normal PLMs and extra PLMs (Figure S1). No extra PLM neurons were observed in *lin-44* mutants or *lin-44 cwn-1 egl-20* mutants.

The Correct Placement of Axons, Growth Cones, and Synapses Requires *lin-17* Function within PLM

lin-44 and *lin-17* mutations affect PLM neuronal development by shortening the anterior process while lengthening the posterior one. This complex phenotype could represent either two different guidance defects in the two processes, or a reversed orientation of the entire PLM cell along the anterior-posterior axis. To better understand these defects, we examined the initial development of PLM in the embryo. PLM neurites begin to grow late in embryogenesis, and the anterior neurite continues to grow rapidly until about 3 hr after hatching (Gallegos and Bargmann, 2004). The anterior neurite then pauses for ∼8 hr before initiating slow maintenance growth to match the growth of the animal. In wild-type embryos observed shortly before hatching, the PLM neuron was already bipolar and had distinct anterior and posterior processes; the anterior PLM process was tipped by a growth cone, but the posterior process was not (Figure 2A). In *lin-44* and *lin-17* mutant embryos, the posterior process was tipped with a growth cone-like structure, but the anterior process usually was not (Figures 2B and 2C). Even at these early stages, the relative lengths of the two processes reflected their final length: wild-type embryos had long anterior PLM processes and short posterior processes, whereas *lin-44* and *lin-17* mutants had short anterior PLM processes and long posterior processes (Figure 2D). Thus, *lin-44* and *lin-17* affected both PLM processes at the earliest observable stages of development.

The embryonic and adult phenotypes in *lin-17* and *lin-44* mutants suggest that the entire PLM neuron is inverted in its anterior-posterior orientation. To further explore this possibility, we examined the localization of the synaptic vesicle protein *snb-1* (synaptobrevin) in PLM (Nonet, 1999). In wild-type animals, a *mec-7::snb-1::GFP* fusion protein is enriched in the anterior branch of PLM where the chemical synapses are formed (Nonet, 1999; and Figure 3A). In *lin-17* and *lin-44* animals, *mec-7::snb-1::GFP* expression was enriched in the PLM posterior process (Figures 3B and 3C), suggesting that both the molecular composition and the morphology of PLM processes are reversed in the Wnt pathway mutants.

Wnt signals could exert direct action on PLM, or they could act indirectly by affecting the overall patterning of the embryo. To determine whether *lin-17* functions cell autonomously in PLM, we expressed a wild-type *lin-17* cDNA selectively in mechanosensory neurons of *lin-17* mutants by using *mec-4* or *mec-7* promoters, which direct expression in PLM, ALM, AVM, and PVM
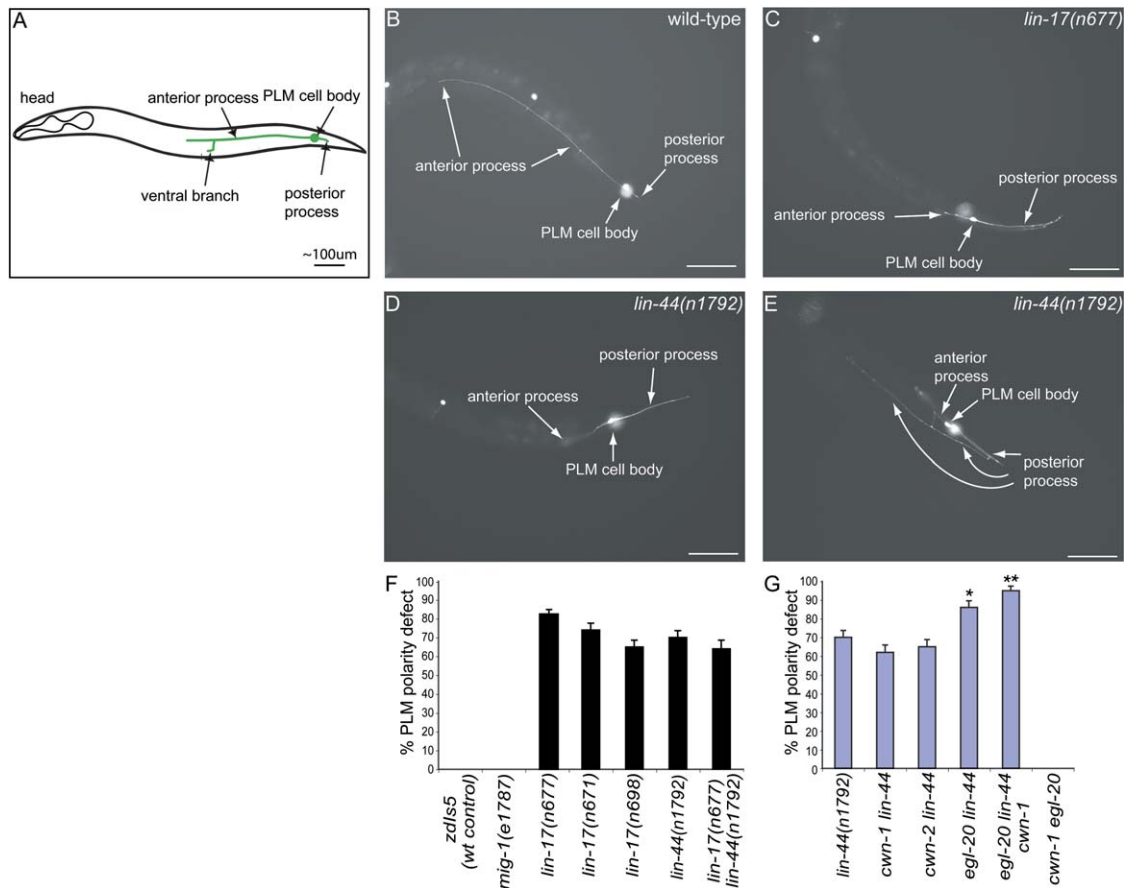
Figure 1. *lin-17* and *lin-44* Affect PLM Development

(A) Morphology of a PLM neuron (green). Only one (the left) of the two symmetric PLM neurons is shown. In all of the figures, anterior is toward the left and dorsal is up.

(B–E) Fluorescence images of PLM neurons of (B) wild-type L4 larva, (C) *lin-17(n677)* L4 larva, and (D and E) *lin-44(n1792)* L4 larvae. In (C) and (D), the anterior PLM process is short, and posterior process is long. In (E), the posterior process reaches the tip of the tail and turns anterior. The scale bar is 50 μm.

(F) Quantitation of PLM defects in *lin-17* and *lin-44* mutants.

(G) Quantitation of PLM defects in Wnt double and triple mutants. *cwn-1*, *cwn-2*, and *egl-20* single mutants did not produce any effect on PLM (data not shown). Error bars indicate the standard error of proportion. *, different from *lin-44* single mutants, p < 0.05; **, different from *lin-44* single mutants, p < 0.01; t test for proportion.

mechanosensory neurons (Lai et al., 1996; Hamelin et al., 1992). *mec-4::lin-17* and *mec-7::lin-17* transgenes were both able to rescue the PLM defects of *lin-17* mutants with high efficiency (Figure 4A). These results suggest that *lin-17* can act autonomously within PLM neurons. *mec-4* and *mec-7* reporter genes are expressed after the division that gives rise to PLM, suggesting that *lin-17* effects on polarity are independent of any earlier lineage defect.

**Delocalized LIN-44 Expression Can Rescue
PLM Development**
During embryonic and postembryonic development, *lin-44* is expressed selectively in the posterior epidermal cells hyp8, hyp9, hyp10, and hyp11 (Herman et al., 1995). These cells are all posterior to the PLM cell body (Figure 4B), suggesting that a directional LIN-44 signal could act instructively to affect PLM morphology. Alternatively, LIN-44 might act as a permissive cue whose source is not central to PLM polarity. To discriminate

between these possibilities, we generated transgenic lines in which a wild-type *lin-44* cDNA was expressed in different patterns in a *lin-44* mutant background.

To disrupt the *lin-44* pattern in the immediate neighborhood of PLM, we expressed a *lin-44* cDNA under an *egl-5* promoter (the *egl-5::lin-44* plasmid was a kind gift from Hitoshi Sawa). In the embryo, the *egl-5* promoter is expressed in several cells posterior to the PLM cell body, in cells anterior to PLM, and in PLM itself (Ferreira et al., 1999). In later stages, *egl-5* is expressed in cells anterior to PLM. The *egl-5::lin-44* transgene partially rescued the PLM defect of *lin-44* mutants despite its altered expression pattern (Figure 4C).

To disrupt the *lin-44* expression pattern more substantially, we expressed a *lin-44* cDNA under a heat shock promoter (*hsp16-2::lin-44*) in a *lin-44* mutant background. The heat shock promoter is broadly expressed in many neuronal and nonneuronal cell types (Stringham et al., 1992). Remarkably, a 10 min 33°C heat shock during embryonic development was sufficient to rescue
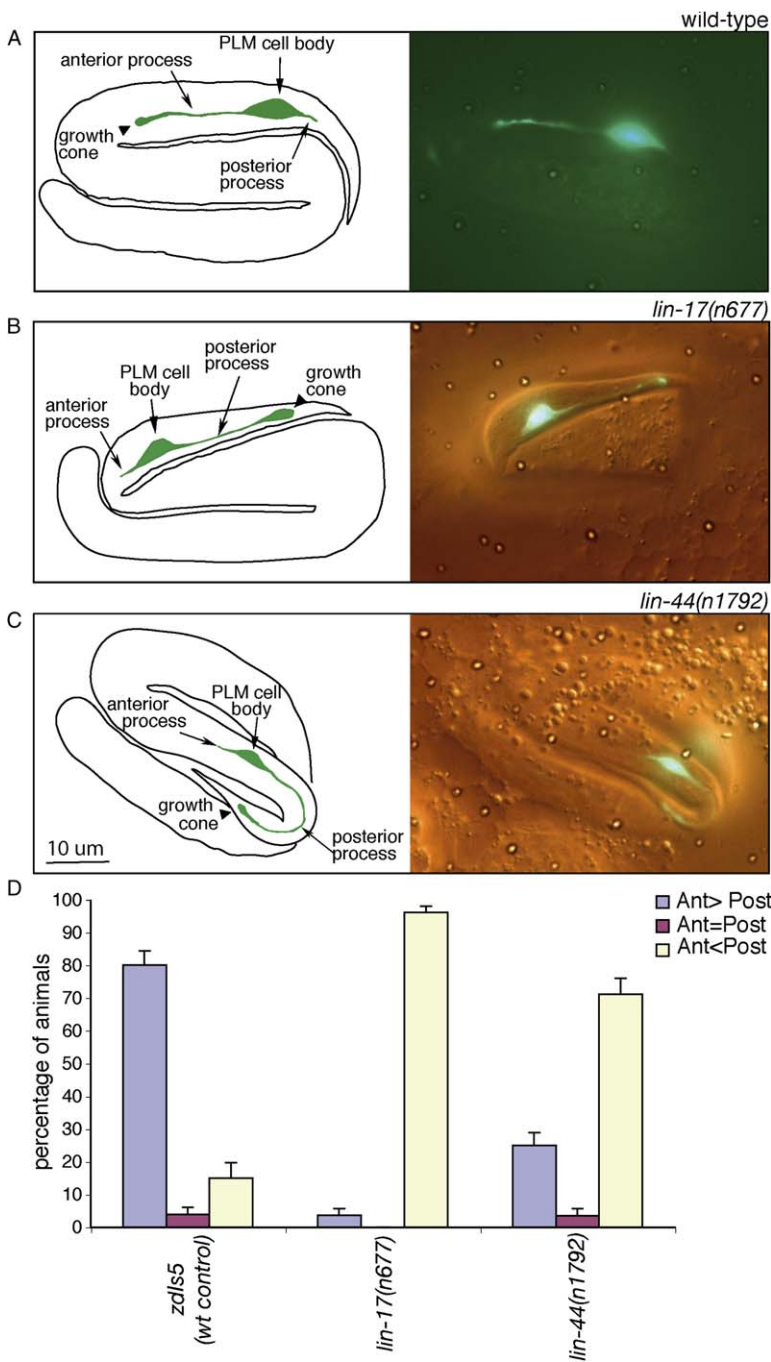
Figure 2. PLM Development in the Embryo

(A) Fluorescence image and diagram of a PLM neuron in a wild-type embryo at 3-fold stage. The nose is at the lower left.

(B and C) DIC-fluorescence images and diagrams of PLM in a (B) *lin-17(n677)* mutant embryo and a (C) *lin-44(n1792)* mutant embryo. The nose is at the left.

(D) Quantitation of relative anterior and posterior PLM process lengths in embryos for wild-type (n = 85), *lin-17(n677)* (n = 79), and *lin-44(n1792)* (n = 84).

Error bars indicate standard error of proportion.

PLM morphology in about half of the mutant animals (Figure 4D). This result suggests that precise posterior expression of *lin-44* is not required for its function. In a wild-type background, a similar pulse of *hsp16-2::lin-44* caused minimal effects on PLM development (Figure 4D).

The *hsp16-2* promoter is expressed at a low level at 25°C (Stringham et al., 1992), and PLM neurons in *lin-44; hsp16-2::lin-44* animals grown continuously at 25°C were partially rescued compared to *lin-44* controls (Figure 4E). We used temperature-shift experiments to determine when *lin-44* acts in development. When animals were shifted to 25°C immediately after the birth of the PLM neurons, we observed significant rescue of PLM polarity. When animals were shifted to 25°C in the L1 stage, no rescue was observed (Figure 4F). These experiments define an interval after PLM birth, but before hatching, in which *lin-44* can function to reorient PLM polarity.

These results indicate that *lin-44* is central to PLM polarity, but that it does not need to be expressed in its normal pattern to function, nor is it the only source of positional information for PLM (see Discussion).

LIN-17 Is Enriched in the Posterior Process of PLM

Frizzled proteins can be asymmetrically localized in dividing cells (Park et al., 2004) or in cells undergoing planar cell polarity (Strutt, 2001). To further characterize the
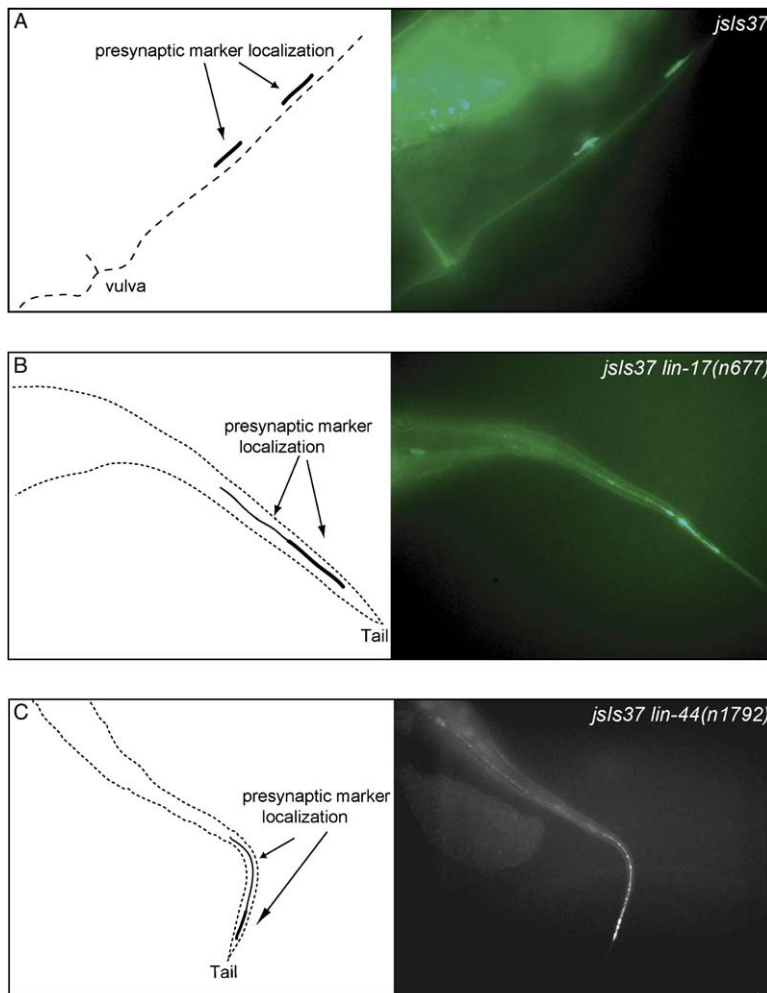
Figure 3. SNB-1::GFP Presynaptic Marker Localization in PLM

(A) Fluorescence image and a diagram of the vulva region in a wild-type animal expressing *mec-7::snb-1::GFP*. PLM vesicle clusters are only visible on the ventral side near the vulva. (B and C) Fluorescence images and diagrams of the tail in (B) *lin-17(n677)* animal or in (C) *lin-44(n1792)* animal expressing *mec-7::snb-1:: GFP*. The synaptic marker is enriched at the tip of the tail, not near the vulva.

intracellular effects of Wnt signaling on PLM neurons, we examined the subcellular localization of LIN-17 in PLM. A C-terminally-tagged LIN-17::mRFP1 fusion protein was able to rescue most of the PLM defects of *lin-17* mutants (Figure 4A). In these rescued animals, and in wild-type animals expressing a *lin-17::mRFP1* transgene, LIN-17::mRFP1 was enriched in the PLM posterior process; in some cases, it also capped the posterior side of the PLM cell body (Figure 5A, and data not shown). The posterior PLM process consistently expressed about three times as much LIN-17::mRFP1 per unit area as the anterior process (Figure 5D).

In a *lin-44* mutant background, LIN-17::mRFP1 was uniformly distributed between the anterior and posterior PLM processes (Figures 5B and 5D), indicating that LIN-17 asymmetry was lost. This result suggests that LIN-44 might regulate PLM neuronal polarity by establishing or maintaining an asymmetric distribution of LIN-17 in the cell.

Whereas overexpression or misexpression of *lin-44* had little effect on PLM neurons, overexpression of *lin-17* disrupted PLM polarity in a wild-type background. *mec-7::lin-17* or *mec-7::lin-17::mRFP1* caused PLM reversals in wild-type animals when they were injected at ten times the rescuing concentration (Figures 5E and 5F). Asymmetric LIN-17::mRFP1 protein localization was

significantly diminished in these overexpressing strains (Figures 5C and 5D). These observations suggest that PLM is highly sensitive to the level of LIN-17 expression for polarity and for the asymmetric localization of LIN-17.

EGL-20 and CWN-1 Regulate ALM Anterior-Posterior Polarity

All known effects of *lin-44* on asymmetric cell division and cell fate occur in the tail of the animal, where PLM is located. This observation is consistent with the restricted localization of *lin-44* expression in the tail, but leaves open the question of how anterior-posterior axon outgrowth is regulated in other body regions. The two ALM mechanosensory neurons' cell bodies are located in the anterior half of the animal (Figures 6A and 6B). Each ALM neuron has a single well-developed process that exits from the anterior side of the cell body and extends into the head. Near the pharynx, each ALM sends a short ventral branch into the nerve ring, where it makes chemical synapses with other classes of neurons (White et al., 1986) (Figure 6B). ALM and PLM share many functions and patterns of gene expression, but *lin-44* and *lin-17* mutations had no effect on ALM development (Figure 6G). However, about 35% of animals with mutations in the two Wnt genes *cwn-1* and *egl-20* had defects in which the single ALM process extended
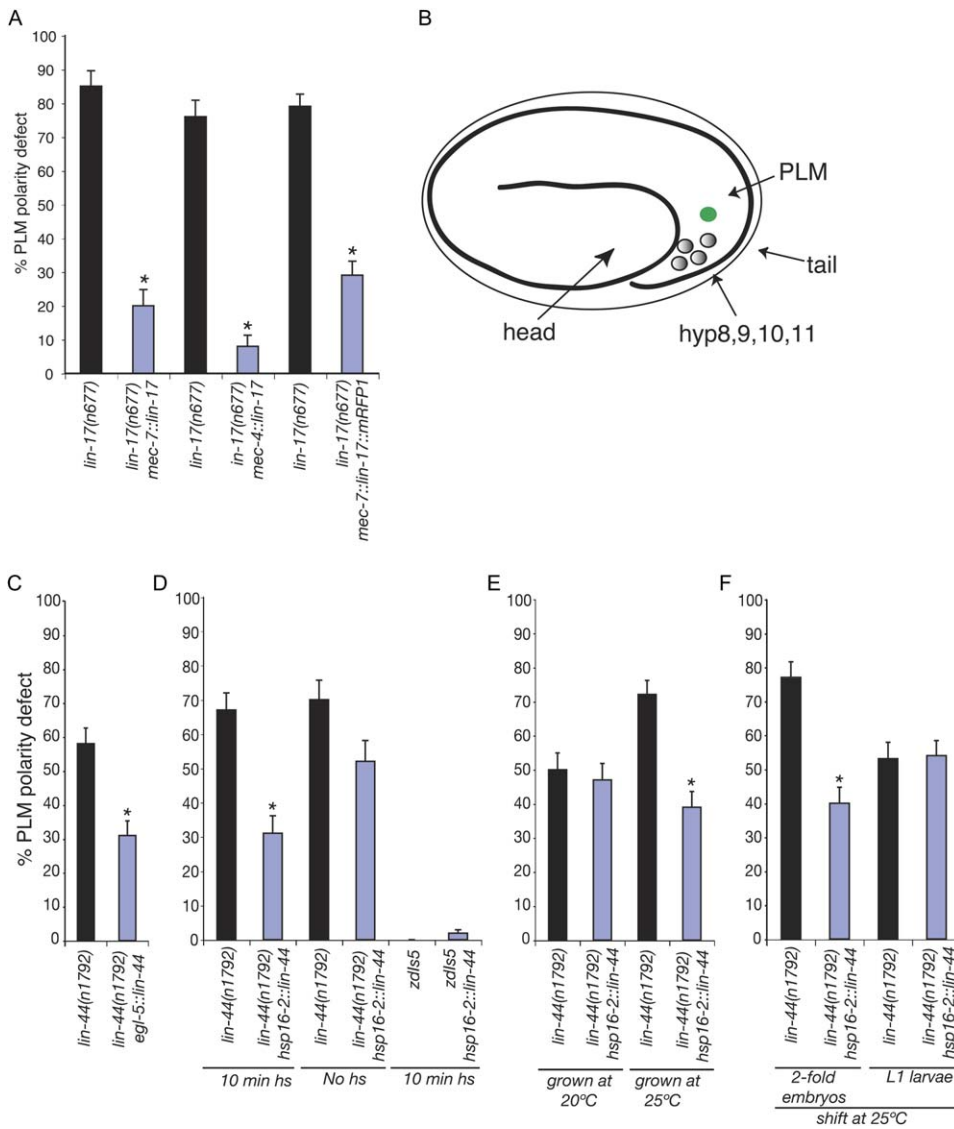
Figure 4. Expression and Misexpression of LIN-17 and LIN-44

(A) Rescue of the PLM polarity defect in *lin-17(n677)* mutant animals carrying *kyEx738(mec-7::lin-17)*, *kyEx739(mec-4::lin-17)*, or *kyEx838(mec-7::lin-17::mRFP1)* transgenes. *, $p < 0.01$ by t test.

(B) Diagram of an embryo at about the 2-fold stage highlighting PLM and the LIN-44-expressing hypodermal cells hyp8, hyp9, hyp10, and hyp11.

(C) Rescue of the *lin-44* PLM defect by the transgene *kyEx1144(egl-5::lin-44)*. *p < 0.01 compared to nontransgenic sibling controls.

(D) Rescue of the *lin-44* PLM defect with the transgene *kyEx765(hs::lin-44)*. Results are from transgenic animals and nontransgenic siblings after 10 min of 33°C heat shock during embryonic development. The transgene did not cause defects in the wild-type (*zdIs5*) background.

(E) Rescue of the *lin-44* PLM defect with the transgene *kyEx1233(hs::lin-44)* by temperature shift. Transgenic animals and nontransgenic siblings, raised at 25°C or 20°C. *, different from nontransgenic siblings, $p < 0.05$ by t test.

(F) *lin-44* can function after PLM is born. *kyEx1233* (*hs::lin-44*) animals were shifted to 25°C either at the 2-fold stage, when PLM is born, or at the L1 stage.

Error bars indicate standard error of proportion.

posteriorly rather than anteriorly from the cell body (Figures 6C and 6D). In many animals, the ALM posterior process turned ventrally in the lumbar commissure in the tail, a morphology reminiscent of the wild-type ALM ventral branch in the nerve ring (Figure 6D). No defects were observed in *cwn-1* or *egl-20* single mutants, and the ALM defect was not enhanced in the triple mutant *lin-44 cwn-1 egl-20* (Figure 6G). Thus, *cwn-1* and *egl-20* are two redundant Wnt proteins that regulate ALM development.

Like the PLM defect in *lin-44* animals, the ALM defect in *cwn-1 egl-20* Wnt mutants was detectable as soon as

the *mec-4::GFP* reporter was expressed in the embryo. In wild-type embryos, the ALM anterior process was tipped with a growth cone that extended toward the head. In *cwn-1 egl-20* double mutants, the ALM process with a growth cone extended posteriorly toward the tail (data not shown).

In wild-type ALM neurons, presynaptic vesicles in the ventral anterior branch of ALM can be visualized by using *mec-7::snb-1::GFP* (Nonet, 1999) (Figure 6E). In *cwn-1 egl-20* double mutant ALM neurons, SNB-1::GFP was frequently enriched in the posterior ALM process, where
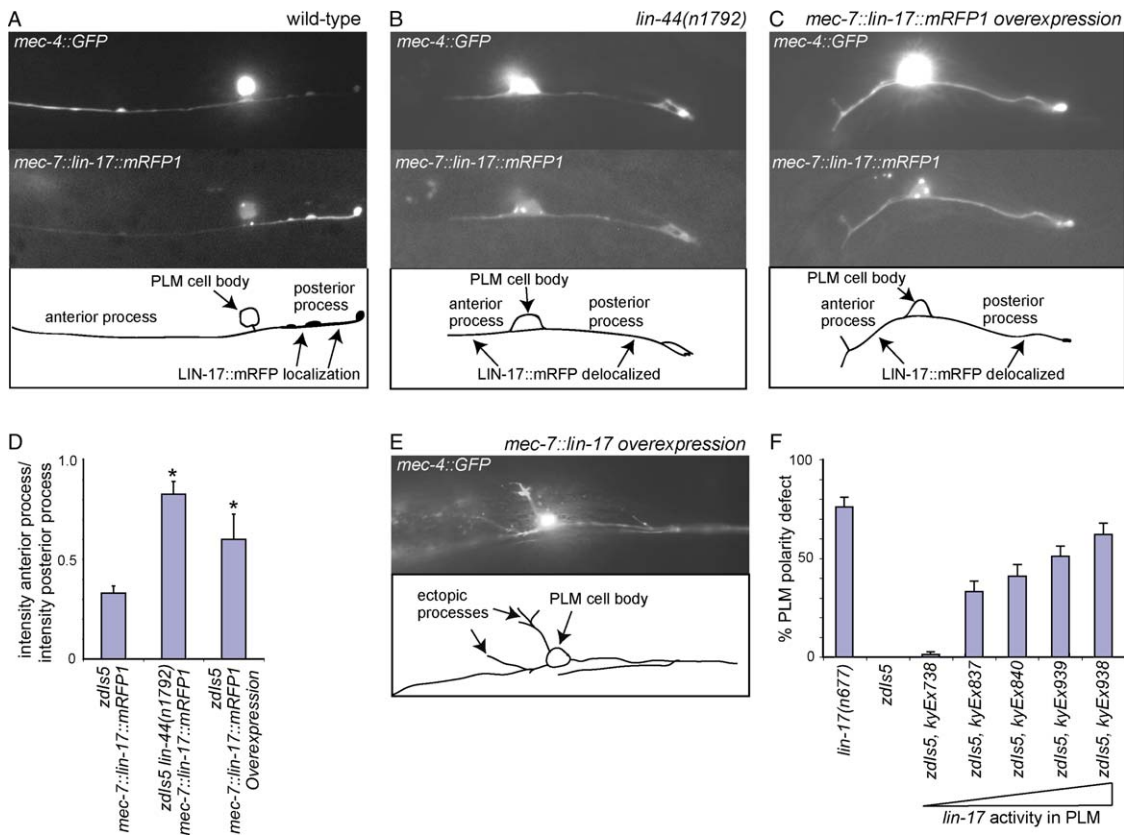
Figure 5. Posterior Localization of LIN-17 in PLM

(A and B) Fluorescence images and diagrams of PLM in (A) wild-type and (B) *lin-44(n1792)* animals expressing the *kyEx838* transgene (*mec-7::lin-17::mRFP1*) and *zdIs5* (*mec-4::GFP*).

(C) Fluorescence images and diagrams of PLM in wild-type animals expressing the *kyEx1235* transgene (*mec-7::lin-17::mRFP1*) and *zdIs5* (*mec-4::GFP*).

(D) Quantitation of LIN-17 localization. Fluorescence intensity ratio of the anterior/posterior processes in wild-type (n = 28) and *lin-44* animals (n = 10) expressing the *kyEx838* transgene (*mec-7::lin-17::mRFP1*), and in wild-type (n = 13) animals with reversed PLM neurons due to overexpression of the *kyEx1235* transgene (*mec-7::lin-17::mRFP1*). *, different from wild-type animals, p < 0.05, Bonferroni t test for proportion.

(E) Fluorescence image and diagram of a PLM defect caused by LIN-17 overexpression. *kyEx939* (*mec-7::lin-17* at 5 ng/µl) in an animal expressing *mec-4::GFP*. The PLM is reversed on the A/P axis. In this animal, additional processes extend from the PLM cell body in random directions (5%–10% penetrance, defect arises mostly after L1 stage).

(F) Quantitation of the PLM polarity defect (reversal) resulting from LIN-17 overexpression. Different transgenic animals carrying *mec-7::lin-17* injected at different concentrations. *kyEx738* (0.1 ng/µl); *kyEx837* and *kyEx840* (1 ng/µl); *kyEx939* and *kyEx938* (5 ng/µl). Error bars indicate standard error of proportion.

it turned ventrally into the lumbar commissure (Figure 6F). These posterior ALM vesicle markers were regularly spaced and punctate, resembling normal ALM synapses. *cwn-1 egl-20* animals had defective behavioral response to anterior touch that correlated closely with ALM polarity reversals (Figure S2).

EGL-20 is normally expressed from epidermal and muscle cells in the posterior region of the animal near the anus (Whangbo and Kenyon, 1999), and thus it could be a directional cue for ALM polarity. To explore this possibility, an *egl-20* cDNA was expressed under the heat shock promoter (Whangbo and Kenyon, 1999) in the *cwn-1 egl-20* double mutant background. A 5 min 33ºC heat shock during embryonic development was able to rescue most of the ALM defects (Figure 6H). However, longer heat shock exposures of 10 and 15 min were significantly less efficient in rescuing the ALM defect. Moreover, the same *hs::egl-20* transgene in a wild-type background induced reversals in ALM polarity after 15 min of heat shock (Figure 6H). These results

suggest that overexpression of delocalized EGL-20 activity can disrupt ALM development.

The potential Frizzled receptor in ALM is unknown; *lin-17* mutants showed no apparent defect in ALM polarity. However, overexpression of LIN-17 from a *mec-7::lin-17* transgene in wild-type animals generated a reversed ALM morphology similar to that of *cwn-1 egl-20* double mutants (Figure 6G). Therefore, altered Frizzled activity can reverse the orientation of ALM neurons, like altered Wnt activity.

Discussion

Axon guidance is typically studied in the context of attractants or repellents that act on the developing growth cone. For example, Wnt5 in flies and Wnt4 in mice act as secreted guidance molecules that direct growth cones along the longitudinal anterior-posterior axis (Yoshikawa et al., 2003; Lyuksyutova et al., 2003). Here, we show that in *C. elegans*, Wnts also pattern
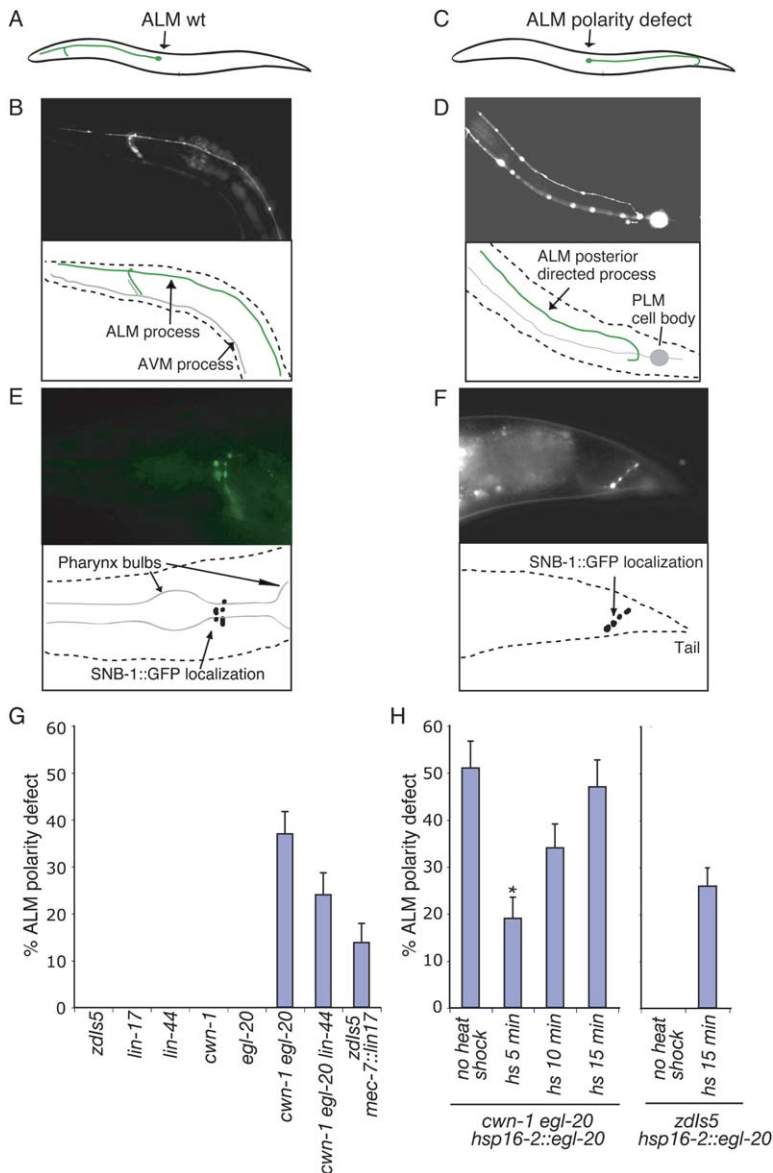
Figure 6. ALM Defect in *cwn-1 egl-20* Double Mutants

(A) Morphology of an ALM neuron (green). Only one (the left) of the two symmetric ALM neurons is shown.

(B) Fluorescence image and diagram of an ALM neuron in a wild-type animal.

(C) Reversed ALM neuron, as observed in *cwn-1 egl-20* double mutants.

(D) Fluorescence image and diagram of an *cwn-1 egl-20* double mutant animal highlighting the ALM process.

(E) Fluorescence image and a diagram of a wild-type animal expressing the *mec-7::snb-1::GFP(jsIs37)* transgene. The presynaptic marker localizes to bright puncta in the nerve ring.

(F) Fluorescence image and a diagram of an *cwn-1 egl-20* double mutant animal expressing the *mec-7::snb-1::GFP(jsIs37)* transgene. The presynaptic marker localizes to bright puncta on the posterior ALM process.

(G) Quantitation of ALM polarity defects. *mec-7::lin-17* overexpression (*kyEx837*) induced ALM polarity reversal and less frequent bipolar ALM morphology (not scored as reversed). n = 60–100 cells per strain.

(H) Left, rescue of the ALM defect in *cwn-1 egl-20* double mutants with the *hs::egl-20* transgene (*muIs53*). *, significant rescue compared to non-heat-shocked control (p < 0.01, n = 76). Right, 33°C heat shock in a wild-type background induced ALM polarity defects. Error bars indicate standard error of proportion.

axon outgrowth along the anterior-posterior axis. In PLM and ALM mechanosensory neurons, Wnts achieve this not by attracting or repelling growth cones, but by inverting the overall anterior-posterior orientation of the neuron and its polarized processes.

The specific expression of LIN-44/Wnt posterior to the PLM cell body suggests that it could function as a directional cue for PLM polarity (Figure 4; Figure S3). The normal PLM morphology could result from an inhibitory relationship in which the long process selects a trajectory away from posterior Wnt. LIN-17 protein is preferentially localized to the posterior PLM process, and LIN-44 is required for the posterior localization of LIN-17 protein in PLM neurons, suggesting that an external posterior Wnt signal is transformed into an internal posterior Frizzled signal in PLM.

Surprisingly, *lin-44* partly rescues PLM when expressed from a heat shock promoter, suggesting that localized *lin-44* expression is not essential to its function. Full rescue is never observed with *egl-5::lin-44* or *hs::lin-44* transgenes, suggesting that the proper spatial and temporal pattern of *lin-44* activity is required for full function. However, any *lin-44* rescue with the heat shock or *egl-5* promoters was unexpected. Indeed, the expected result for such a transgene is disruption of wild-type development, as we observed in ALM after ubiquitous *egl-20* expression. In the extreme, Wnt signaling could be permissive for reorientation of PLM polarity. Based on heat shock experiments, the Wnt EGL-20 was suggested to have a permissive role in the polarity of the V5 asymmetric cell division and the anterior-posterior migration of the Q neuroblast (Whangbo et al., 2000; Whangbo and Kenyon, 1999).

Positional information that requires Frizzled, but not Wnts, is central to *Drosophila* planar cell polarity, and many features of LIN-17 signaling in PLM are similar to those of Frizzled in PCP. PCP is highly sensitive to Frizzled overexpression, as PLM polarity is sensitive to LIN-17 overexpression (Adler et al., 1997). PCP requires asymmetric subcellular localization of Frizzled, and this

asymmetric distribution is reinforced by positive feedback through the PCP pathway (Usui et al., 1999; Strutt, 2001); PLM polarity is associated with asymmetric subcellular localization of LIN-17, which is regulated by LIN-44 signaling. Another *C. elegans* Frizzled molecule that echoes PCP is MOM-5, which is asymmetrically localized to the posterior side of many dividing cells in the embryo (Park et al., 2004). During PCP in the *Drosophila* eye, positional information is provided by several cadherin-related proteins that drive Frizzled localization to one side of the developing photoreceptor neurons (Yang et al., 2002). It will be interesting to see whether cadherin-related proteins have a role in LIN-17 localization in PLM.

PLM polarity is clearly Wnt dependent, unlike *Drosophila* PCP. In any model, LIN-17 requires a threshold level of Wnt activation, normally provided by LIN-44, to maintain posterior localization and regulate PLM polarity.

Could *lin-44* still provide positional information to PLM? It is possible that delocalized *lin-44* expression is shaped into a spatial pattern by extracellular Wnt binding proteins, Wnt inhibitors, or directed Wnt transport (Greco et al., 2001; Leyns et al., 1997; Bejsovec and Wieschaus 1995). Differential use of protein modification pathways might predispose posterior cells to express LIN-44 at higher levels than anterior cells (Kadowaki et al., 1996; van den Heuvel et al., 1993, Rocheleau et al., 1997). Perhaps PLM reads the pattern generated by all three Wnts, not just LIN-44. *egl-20* and *cwn-1* are expressed mostly anterior to the PLM cell body (Herman et al., 1995; Whangbo and Kenyon, 1999; Pan et al., 2006 [this issue of *Developmental Cell*]); the three Wnts LIN-44, EGL-20, and CWN-1 might all contribute to the patterned Wnt activity that PLM uses to orient itself on the anterior-posterior axis.

ALM development and PLM development have interesting similarities and differences that help clarify the role of Wnts in orienting polarity. The phenotypic effects of Wnt mutations on ALM and PLM morphology are remarkably similar, and they are most consistent with inversion of cell polarity along the longitudinal axis. However, PLM development is strongly affected by *lin-44*, with a minor role from the Wnt genes *egl-20* and *cwn-1*; the more anterior ALM neurons are strongly affected by the more anterior Wnt ligands *egl-20* and *cwn-1*, but not by *lin-44*. These observations suggest that different sets of (partly redundant) Wnt genes preferentially regulate either specific groups of cells or specific regions of the body. The expression pattern of the Wnts is consistent with functions in different body regions.

ALM polarity was reversed in wild-type animals after ubiquitous expression of *egl-20*, strongly suggesting that ALM normally reads positional information from posterior Wnts to choose an anterior direction. The cellular sources of *egl-20* and *cwn-1* are far posterior to ALM, so it may be easier to create a biologically significant disruption of Wnt expression patterns near ALM than is possible near PLM, where endogenous Wnts are expressed at higher levels.

The results from this work and the accompanying paper provide a broad view into the effects of Wnts on anterior-posterior patterning of the nervous system.

Wnts act as anterior-posterior cues for developing axons across a single segment in *Drosophila*, or across the body axis in *C. elegans* and vertebrates. Wnts can affect growth cone turning in *C. elegans*, as they do in *Drosophila* and vertebrates (Pan et al., 2006; Yoshikawa et al., 2003; Lyuksyutova et al., 2003; Liu et al., 2005; M.A.H., unpublished data). However, they can also provide information for earlier events such as cell migration and the orientation of polarity (Pan et al., 2006; this paper). The identification of Wnt mutants in a variety of screens reveals a fundamental role in organization of the anterior-posterior body axis.

One surprising feature of PLM development is that the absence of *lin-17* and *lin-44* leads to a great excess of complete PLM reversals, rather than to a random mixture of reversed and normal PLMs. Similarly, the asymmetric cell divisions of T and B neuroblasts are usually reversed in *lin-44* mutants (Herman and Horvitz, 1994; Herman et al., 1995). These results suggest that the Wnt-Fz pathway antagonizes another mechanism that biases polarity in the opposite direction. This bias could result from a discrete signaling molecule, an intrinsic determinant from the last cell division, or a more permissive axon growth environment posterior to PLM. The idea of Wnts acting to reorient neuronal polarity is similar to the idea that Wnts reorient the centrosome and mitotic spindle during asymmetric cell divisions (Thorpe et al., 1997). The centrosome correlates with the site of future axon growth in many neurons (Lefcort and Bentley 1989; Zmuda and Rivas, 1998; de Anda et al., 2005), so the underlying mechanisms that Wnts use to orient neuronal polarity and asymmetric cell divisions could be the same.

Experimental Procedures

Strains

Nematodes were cultured by using standard techniques (Brenner, 1974). All experiments were performed at 20ºC. The following mutations were used: LGI, *lin-17(n677)*, *lin-17(n671)*, *lin-17(n698)*, *mig-1(e1787)*, *lin-44(n1792)*; LGII, *cwn-1(ok546)*; LGIV, *egl-20(n585)*, *cwn-2(ok895)*; LGV, *cfz-2(ok1201)*. Transgenes were *zdIs5[mec-4:: GFP, lin-15(+)]*; *jsIs37[mec-7::snb-1::GFP]*; *muIs53[hsp16-2::egl-20 + unc-22 antisense]*; *kyEx765[hsp16-2::lin-44 (20 ng/µl), odr-1:: dsRED (30 ng/µl)]*; *kyEx1233[hsp16-2::lin-44 (10 ng/µl), odr-1::dsRED (40 ng/µl)]*; *kyEx738[mec-7::lin-17 (0.1 ng/µl), odr-1::dsRED (25 ng/µl)]*; *kyEx739[mec-4::lin-17 (1 ng/µl), odr-1::dsRED (25 ng/ µl)]*; *kyEx838[mec-7::lin-17::mRFP1 (0.1 ng/µl), odr-1::dsRED (30 ng/µl)]*; *kyEx1235[mec-7::lin-17::mRFP1 (1 ng/µl), odr-1::dsRED (30 ng/µl)]*; *kyEx837 and kyEx840[mec-7::lin-17 (1 ng/µl), odr-1:: dsRED (30 ng/µl)]*; *kyEx938 and kyEx939[mec-7::lin-17 (5 ng/µl), odr-1::dsRED (30 ng/µl)]*; *kyEx1144[egl-5::lin-44 (30 ng/µl), odr-1::dsRED (30 ng/µl)]*. The *zdIs5* strain was provided by Scott Clark, the *jsIs37* strain was provided by Mike Nonet, the *muIs53* strain was provided by Cynthia Kenyon, the *gpa-10::GFP* strain was provided by Gert Jansen, and the *mec-17::GFP* and *mec-18::GFP* strains were provided by Marty Chalfie.

Molecular Biology

Standard molecular biology techniques were used. *mec-7::lin-17* and *mec-4::lin-17* plasmids were generated by using an XmaI/KpnI fragment from a *lin-17* cDNA clone (yk496g4, a gift from Yuji Kohara) and were inserted behind the *mec-7* promoter (pPD96.41, a gift from Andrew Fire) or behind the *mec-4* promoter. Sequence analysis revealed that the *lin-17* cDNA retained the seventh intron.

The *mec-7::lin-17::mRFP1* plasmid was prepared by using a PCR fusion approach (Hobert, 2002). A *lin-17* cDNA PCR fragment was amplified by using a 5′ primer containing an XmaI site (5′-CGGGCC

CGGGATGATGCATTCTTTGGGCAT-3′) and a 3′ primer containing a region homologous to the 5′ end of *mRFP1* (5′-ACGTCCTCGGAG GAGGCCATGACGACCTTACTGGGTCTCC-3′). A different PCR product was obtained amplifying *mRFP1* by using a 5′ primer containing a region homologous to the *lin-17* cDNA 3′ end (5′-GGAGACCCAG TAAGGTCGTCATGGCCTCCTCCGAGGACGT-3′) and a 3′ primer containing a KpnI site (5′-CGGGGTACCTTAGGCGCCGGTGGAGTG GC-3′). A final third PCR product was obtained by using the 5′ primer of the *LIN-17* fragment and the 3′ primer of the *mRFP1* fragment and by using as template a small amount of each of the two initial PCR products (1 μl of 1/10 dilution). The resulting PCR fusion fragment containing *lin-17* cDNA fused in frame with *mRFP1* had an XmaI site at the 5′ end and a KpnI site at the 3′ end and was cloned into the pPD96.41 vector.

The *hsp16-2::lin-44* plasmid was prepared by using a *lin-44* cDNA obtained as a gift from Yuji Kohara (yk120c7). PCR primers to amplify *lin-44* were designed so that the PCR fragment contained an NheI site at the 5′ end (5′-CCGGGGCCCGCTAGCATGCGAGCAGCTCCT TTTG-3′) and a SacI site at the 3′ end (5′CCGGGCGAGCTCTTAAAA AATTAGGCTTTTCGGCGG-3′), and the product was ligated into pPD49.78. The transgene shown in Figure 4D had a mutation that resulted in the addition of 20 C-terminal amino acids to LIN-44. The transgene shown in Figures 4E and 4F, which gave similar results, encoded an intact LIN-44 protein.

Scoring of PLM/ALM Processes

The processes of PLM/ALM were visualized by using the integrated *mec-4::GFP* transgene (*zdIs5*). PLM polarity was considered reversed when the anterior process of PLM did not elongate over one-fourth of the animal's body length and the PLM posterior extended to the tip of the tail. In *lin-17* and *lin-44* animals, the polarity defect was often associated with a cell shape/morphology defect, with the cell body becoming more elongated; this phenotype was not studied in detail. In *lin-17*, but not *lin-44*, animals a cell fate defect produced extra PLM cells in about 30% of the scored animals. These cells were also scored and were included in the total; see Figure S1. ALM processes were considered reversed when the unique process was directed to the posterior. In *cwn-1 egl-20* double mutants, in *lin-17* overexpressing animals, and in *hs::egl-20* experiments, we occasionally observed ALM extending a posterior process in addition to the normal anterior one. These animals were not scored as reversed, but were included in the total.

Heat Shock Experiments

Experiments with *hsp16-2::lin-44* and *hsp16-2::egl-20* were performed on eggs collected after bleaching adult hermaphrodites. A 33ºC heat shock was given with a PCR machine. The plates were then incubated at 20ºC, and the animals were scored as L4 or young adults. Alternatively, larvae were placed on a seeded plate and were incubated at 15ºC or 25ºC for one generation, and their progeny were scored at the L4 or adult stage.

Microscopy

Animals were mounted on 4% agar pads in water containing 5 mM sodium azide and were examined by using a Zeiss Axioskop equipped with epifluorescence and DIC. Images were collected by using a Zeiss Axiocam digital camera. The images of LIN-17::mRFP1 localization were collected by using a RTE/CCD-1300 Y/HS Roper Camera.

Fluorescence Measurements

Fluorescence measurements of the PLM processes were taken with Metamorph software. A complete set of images (z-stack) was collected for each animal analyzed. A subset of these in which PLM and its processes were in focus was selected. These images were summed in one image, and fluorescence background was subtracted. A line tool was then used to follow the anterior and posterior processes, the average fluorescence for each process was measured, and the anterior/posterior ratio was calculated for Figure 5D.

Statistical Tests

The t test for proportion (hypothesis test for proportion) was used in all cases, except in those with multiple comparisons, for which the Bonferroni t test was used.

Supplemental Data

Supplemental Data showing effect on PLM fate, behavioral analysis of Wnt and Fz mutants, and models for Wnt regulation of polarity are available at http://www.developmentalcell.com/cgi/content/full/ 10/3/379/DC1/.

References

Adler, P.N., Krasnow, R.E., and Liu, J. (1997). Tissue polarity points from cells that have higher Frizzled levels towards cells that have lower Frizzled levels. Curr. Biol. *7*, 940–949.

Bejsovec, A., and Wieschaus, E. (1995). Signaling activities of the *Drosophila* wingless gene are separately mutable and appear to be transduced at the cell surface. Genetics *139*, 309–320.

Bhanot, P., Brink, M., Samos, C.H., Hsieh, J.C., Wang, Y., Macke, J.P., Andrew, D., Nathans, J., and Nusse, R. (1996). A new member of the frizzled family from *Drosophila* functions as a Wingless receptor. Nature *382*, 225–230.

Bhat, K.M. (1998). *frizzled* and *frizzled 2* play a partially redundant role in wingless signaling and have similar requirements to wingless in neurogenesis. Cell *95*, 1027–1036.

Brenner, S. (1974). The genetics of *Caenorhabditis elegans*. Genetics *77*, 71–94.

Brose, K., Bland, K.S., Wang, K.H., Arnott, D., Henzel, W., Goodman, C.S., Tessier-Lavigne, M., and Kidd, T. (1999). Slit proteins bind Robo receptors and have an evolutionarily conserved role in repulsive axon guidance. Cell *96*, 795–806.

Chen, C.M., and Struhl, G. (1999). Wingless transduction by the Frizzled and Frizzled2 proteins of *Drosophila*. Development *126*, 5441–5452.

Ch'ng, Q., Williams, L., Lie, Y.S., Sym, M., Whangbo, J., and Kenyon, C. (2003). Identification of genes that regulate a left-right asymmetric neuronal migration in *Caenorhabditis elegans*. Genetics *164*, 1355–1367.

de Anda, F.C., Pollarolo, G., Da Silva, J.S., Camoletto, P.G., Feiguin, F., and Dotti, C.G. (2005). Centrosome localization determines neuronal polarity. Nature *436*, 704–708.

Ferreira, H.B., Zhang, Y., Zhao, C., and Emmons, S.W. (1999). Patterning of *Caenorhabditis elegans* posterior structures by the Abdominal-B homolog, egl-5. Dev. Biol. *207*, 215–228.

Gallegos, M.E., and Bargmann, C.I. (2004). Mechanosensory neurite termination and tiling depend on SAX-2 and the SAX-1 kinase. Neuron *44*, 239–249.

Greco, V., Hannus, M., and Eaton, S. (2001). Argosomes: a potential vehicle for the spread of morphogens through epithelia. Cell *106*, 633–645.

Gubb, D., and Garcia-Bellido, A. (1982). A genetic analysis of the determination of cuticular polarity during development in *Drosophila melanogaster*. J. Embryol. Exp. Morphol. *68*, 37–57.

Guo, N., Hawkins, C., and Nathans, J. (2004). Frizzled6 controls hair patterning in mice. Proc. Natl. Acad. Sci. USA 101, 9277–9281.

Hamelin, M., Scott, I.M., Way, J.C., and Culotti, J.G. (1992). The mec-7 β-tubulin gene of Caenorhabditis elegans is expressed primarily in the touch receptor neurons. EMBO J. 11, 2885–2893.

Hao, J.C., Yu, T.W., Fujisawa, K., Culotti, J.G., Gengyo-Ando, K., Mitani, S., Moulder, G., Barstead, R., Tessier-Lavigne, M., and Bargmann, C.I. (2001). C. elegans slit acts in midline, dorsal-ventral, and anterior-posterior guidance via the SAX-3/Robo receptor. Neuron 32, 25–38.

Harris, J., Honigberg, L., Robinson, N., and Kenyon, C. (1996). Neuronal cell migration in C. elegans: regulation of Hox gene expression and cell position. Development 122, 3117–3131.

Hedgecock, E.M., Culotti, J.G., and Hall, D.H. (1990). The unc-5, unc-6, and unc-40 genes guide circumferential migrations of pioneer axons and mesodermal cells on the epidermis in C. elegans. Neuron 4, 61–85.

Heisenberg, C.P., Tada, M., Rauch, G.J., Saude, L., Concha, M.L., Geisler, R., Stemple, D.L., Smith, J.C., and Wilson, S.W. (2000). Silberblick/Wnt11 mediates convergent extension movements during zebrafish gastrulation. Nature 405, 76–81.

Herman, M.A., and Horvitz, H.R. (1994). The Caenorhabditis elegans gene lin-44 controls the polarity of asymmetric cell divisions. Development 120, 1035–1047.

Herman, M.A., Vassilieva, L.L., Horvitz, H.R., Shaw, J.E., and Herman, R.K. (1995). The C. elegans gene lin-44, which controls the polarity of certain asymmetric cell divisions, encodes a Wnt protein and acts cell nonautonomously. Cell 83, 101–110.

Hobert, O. (2002). PCR fusion-based approach to create reporter gene constructs for expression analysis in transgenic C. elegans. Biotechniques 32, 728–733.

Inoue, T., Oz, H.S., Wiland, D., Gharib, S., Deshpande, R., Hill, R.J., Katz, W.S., and Sternberg, P.W. (2004). C. elegans LIN-18 is a Ryk ortholog and functions in parallel to LIN-17/Frizzled in Wnt signaling. Cell 118, 795–806.

Ishii, N., Wadsworth, W.G., Stern, B.D., Culotti, J.G., and Hedgecock, E.M. (1992). UNC-6, a laminin-related protein, guides cell and pioneer axon migrations in C. elegans. Neuron 9, 873–881.

Ishikawa, T., Tamai, Y., Zorn, A.M., Yoshida, H., Seldin, M.F., Nishikawa, S., and Taketo, M.M. (2001). Mouse Wnt receptor gene Fzd5 is essential for yolk sac and placental angiogenesis. Development 128, 25–33.

Kadowaki, T., Wilder, E., Klingensmith, J., Zachary, K., and Perrimon, N. (1996). The segment polarity gene porcupine encodes a putative multitransmembrane protein involved in Wingless processing. Genes Dev. 10, 3116–3128.

Kennedy, T.E., Serafini, T., de la Torre, J.R., and Tessier-Lavigne, M. (1994). Netrins are diffusible chemotropic factors for commissural axons in the embryonic spinal cord. Cell 78, 425–435.

Kennerdell, J.R., and Carthew, R.W. (1998). Use of dsRNA-mediated genetic interference to demonstrate that frizzled and frizzled 2 act in the wingless pathway. Cell 95, 1017–1026.

Kidd, T., Bland, K.S., and Goodman, C.S. (1999). Slit is the midline repellent for the robo receptor in Drosophila. Cell 96, 785–794.

Lai, C.C., Hong, K., Kinnell, M., Chalfie, M., and Driscoll, M. (1996). Sequence and transmembrane topology of MEC-4, an ion channel subunit required for mechanotransduction in Caenorhabditis elegans. J. Cell Biol. 133, 1071–1081.

Lefcort, F., and Bentley, D. (1989). Organization of cytoskeletal elements and organelles preceding growth cone emergence from an identified neuron in situ. J. Cell Biol. 108, 1737–1749.

Leyns, L., Bouwneester, T., Kim, S.H., Piccolo, S., and De Robertis, E.M. (1997). Frzb-1 is a secreted antagonist of Wnt signaling expressed in the Spemann organizer. Cell 88, 747–756.

Lin, R., Hill, R.J., and Priess, J.R. (1998). POP-1 and anterior-posterior fate decisions in C. elegans embryos. Cell 92, 229–239.

Liu, Y., Shi, J., Lu, C.C., Wang, Z.B., Lyuksyutova, A.I., Song, X., and Zou, Y. (2005). Ryk-mediated Wnt repulsion regulates posterior-directed growth of corticospinal tract. Nat. Neurosci. 8, 1151–1159.

Lyuksyutova, A.I., Lu, C.C., Milanesio, N., King, L.A., Guo, N., Wang, Y., Nathans, J., Tessier-Lavigne, M., and Zou, Y. (2003). Anterior-posterior guidance of commissural axons by Wnt-frizzled signaling. Science 302, 1984–1988.

Maloof, J.N., Whangbo, J., Harris, J.M., Jongeward, G.D., and Kenyon, C. (1999). A Wnt signaling pathway controls hox gene expression and neuroblast migration in C. elegans. Development 126, 37–49.

Nonet, M.L. (1999). Visualization of synaptic specializations in live C. elegans with synaptic vesicle protein-GFP fusions. J. Neurosci. Methods 89, 33–40.

Pan, C.L., Howell, J.E., Clark, S.G., Hilliard, M., Cordes, S., Bargmann, C.I., and Garriga, G. (2006). Multiple Wnts and Frizzled receptors regulate anteriorly directed cell and growth cone migrations in Caenorhabditis elegans. Dev. Cell 10, this issue, 367–377.

Park, F.D., Tenlen, J.R., and Priess, J.R. (2004). C. elegans MOM-5/frizzled functions in MOM-2/Wnt-independent cell polarity and is localized asymmetrically prior to cell division. Curr. Biol. 14, 2252–2258.

Rocheleau, C.E., Downs, W.D., Lin, R., Wittmann, C., Bei, Y., Cha, Y.H., Ali, M., Priess, J.R., and Mello, C.C. (1997). Wnt signaling and an APC-related gene specify endoderm in early C. elegans embryos. Cell 90, 707–716.

Sawa, H., Lobel, L., and Horvitz, H.R. (1996). The Caenorhabditis elegans gene lin-17, which is required for certain asymmetric cell divisions, encodes a putative seven-transmembrane protein similar to the Drosophila frizzled protein. Genes Dev. 10, 2189–2197.

Schlesinger, A., Shelton, C.A., Maloof, J.N., Meneghini, M., and Bowerman, B. (1999). Wnt pathway components orient a mitotic spindle in the early Caenorhabditis elegans embryo without requiring gene transcription in the responding cell. Genes Dev. 13, 2028–2038.

Sternberg, P.W., and Horvitz, H.R. (1988). lin-17 mutations of Caenorhabditis elegans disrupt certain asymmetric cell divisions. Dev. Biol. 130, 67–73.

Stringham, E.G., Dixon, D.K., Jones, D., and Candido, E.P. (1992). Temporal and spatial expression patterns of the small heat shock (hsp16) genes in transgenic Caenorhabditis elegans. Mol. Biol. Cell 3, 221–233.

Strutt, D.I. (2001). Asymmetric localization of frizzled and the establishment of cell polarity in the Drosophila wing. Mol. Cell 7, 367–375.

Thorpe, C.J., Schlesinger, A., Carter, J.C., and Bowerman, B. (1997). Wnt signaling polarizes an early C. elegans blastomere to distinguish endoderm from mesoderm. Cell 90, 695–705.

Usui, T., Shima, Y., Shimada, Y., Hirano, S., Burgess, R.W., Schwarz, T.L., Takeichi, M., and Uemura, T. (1999). Flamingo, a seven-pass transmembrane cadherin, regulates planar cell polarity under the control of Frizzled. Cell 98, 585–595.

van den Heuvel, M., Harryman-Samos, C., Klingensmith, J., Perrimon, N., and Nusse, R. (1993). Mutations in the segment polarity genes wingless and porcupine impair secretion of the wingless protein. EMBO J. 12, 5293–5302.

Vinson, C.R., and Adler, P.N. (1987). Directional non-cell autonomy and the transmission of polarity information by the frizzled gene of Drosophila. Nature 329, 549–551.

Vinson, C.R., Conover, S., and Adler, P.N. (1989). A Drosophila tissue polarity locus encodes a protein containing seven potential transmembrane domains. Nature 338, 263–264.

Wehrli, M., and Tomlinson, A. (1995). Epithelial planar polarity in the developing Drosophila eye. Development 121, 2451–2459.

Wehrli, M., and Tomlinson, A. (1998). Independent regulation of anterior/posterior and equatorial/polar polarity in the Drosophila eye; evidence for the involvement of Wnt signaling in the equatorial/polar axis. Development 125, 1421–1432.

Whangbo, J., and Kenyon, C. (1999). A Wnt signaling system that specifies two patterns of cell migration in C. elegans. Mol. Cell 4, 851–858.

Whangbo, J., Harris, J., and Kenyon, C. (2000). Multiple levels of regulation specify the polarity of an asymmetric cell division in C. elegans. Development 127, 4587–4598.

White, J.G., Southgate, E., Thomson, J.N., and Brenner, S. (1986). The structure of the nervous system of the nematode *C. elegans*. Philos. Trans. R. Soc. Lond. B Biol. Sci. *314*, 1–340.

Yang, C.H., Axelrod, J.D., and Simon, M.A. (2002). Regulation of Frizzled by fat-like cadherins during planar polarity signaling in the *Drosophila* compound eye. Cell *108*, 675–688.

Yoshikawa, S., McKinnon, R.D., Kokel, M., and Thomas, J.B. (2003). Wnt-mediated axon guidance via the *Drosophila* Derailed receptor. Nature *422*, 583–588.

Zheng, L., Zhang, J., and Carthew, R.W. (1995). frizzled regulates mirror-symmetric pattern formation in the *Drosophila* eye. Development *121*, 3045–3055.

Zmuda, J.F., and Rivas, R.J. (1998). The Golgi apparatus and the centrosome are localized to the sites of newly emerging axons in cerebellar granule neurons in vitro. Cell Motil. Cytoskeleton *41*, 18–38.